北海道大学工学部研究報告
第130号（昭和61年）

Bulletin of the Faculty of Engineering,
Hokkaido University, No. 130 (1986)

Statistical Properties of Optical Fiber Speckles

Masaaki IMAI*

(Received November 20, 1985)

Abstract

Speckle patterns in the far-field plane as well as the near-field plane (the exit end face) of a multimode fiber through which coherent light propagates are studied mainly from the average contrast and the probability density function of the speckle intensity. These first-order statistics of the speckle intensity are shown as a function of the fiber length, the source bandwidth, and the radial distance in the far-and near-field speckle patterns. The second-order statistics of the speckle intensities at the two points are also discussed on the basis of a conventional speckle theory. Dynamic speckles corresponding to time-varying properties of the speckle pattern are analyzed in conjunction with the modal noise which gives rise to unwanted fluctuations of the transmitted power in the presence of the mode-selective loss, for example, in a misaligned connector.

1. Introduction

A random grannular intensity distribution is observed in the near-field as well as the far-field regions of the exit end of a multimode fiber through which the coherent light such as a laser beam propagates. This random intensity distribution is called a speckle pattern[1]. The speckle pattern in optical fibers is produced by random interference between various modes guided by the fiber[2,3]. The light field launched into the optical fiber is divided into discrete modes and propagates with a definite phase relationship. At the exit end of the fiber, a certain amount of the phase difference is produced among different modes which have different path lengths due to the difference of their angles between the direction of propagation and the guide axis. Whenever such an intermode path difference does not exceed the coherence length of the light source[4-6], the light emerging from the fiber exit end results in a complicated interference among a number of mode fields. This phenomenon yields the random distributions of phase and amplitude of the field, and leads to a speckle pattern.

In the above manner, the speckle formation and the modal distribution are closely related with each other. The fundamentals of the fiber speckle and its statistical properties are briefly reviewed in this article. The first-order statistics of speckle, such as the average contrast and the probability density function of the speckle intensity obtained at a single point in space[7-12], will be first treated. The second-order statistics that are the joint statistical properties of the speckle intensities at two or more points are next discussed on the basis of the speckle theory[13]. Then, the modal noise[14-16] is introduced which is caused

* Department of Engineering Science, Faculty of Engineering, Hokkaido University, Sapporo 060, Japan

by dynamic changes in the speckle pattern. The theoretical background for the modal noise is examined from different speckle regimes. A dynamic variation of speckles causes unwanted intensity modulation of the light passing through the point of speckle-selective loss such as a misaligned fiber-to-fiber joint. The loss fluctuations are finally evaluated using the signal-to-noise ratio which is a reciprocal of the average contrast defined in the speckle pattern.

2. Modes and speckle pattern

In general, the number of speckles is proportional to the number of modes guided by an optical fiber[14-16]. Let us consider, for example, a fiber through which only two modes of the highest and lowest orders can propagate. The intensity distribution across the core of the fiber shows a regular fringe pattern due to interference between two wavefronts of dotted lines as illustrated in Fig. 1. Each fringe corresponds to a single speckle and there are several fringes for only two modes. The highest-order mode undergoes a critical angle $\theta=\sin^{-1}(NA)$ in which $NA=(n_1^2-n_2^2)^{1/2}$ indicates the numerical aperture, n_1 and n_2 being the refractive indices of core and cladding, respectively. Therefore, the smallest speckle size Δx may be given approximately by half the fringe spacing, i. e.,

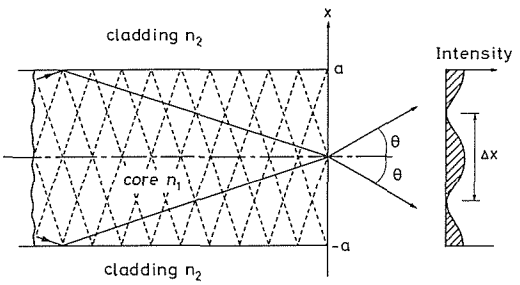

Fig. 1 Interference of the lowest- and highest-order modes which propagate at the low-grazing angle and the critical angle in an optical fiber, respectively.

$$\Delta x=\lambda/2(NA). \tag{1}$$

When all the modes with intermediate angles contribute to interference, the light with lower spatial frequencies could be superimposed on the fringe. But the finest structure of the fringe pattern is determined by the size of Δx. The speckle size also determines the total number N of two-dimensional speckles, contained in the cross section of a cylindrical fiber, and yields

$$N=\pi(a/\Delta x)^2=\pi(2a(NA)/\lambda)^2, \tag{2}$$

where λ is the wavelength of light and a is the core radius. This number of speckles is almost indentical with the number of guided modes supported by a step-index fiber[17] which is given by

$$N=2(\pi a(NA)/\lambda)^2. \tag{3}$$

The similarities of the number of modes and speckles are obvious from Eqs. (2) and (3). The number of the modes increases with an increase of the numerical aperture of a fiber or of the ratio of the core diameter to the wavelength of light. Thus, the fiber with a large core diameter and a high NA exhibits a great number of speckles. It is also apparent that an

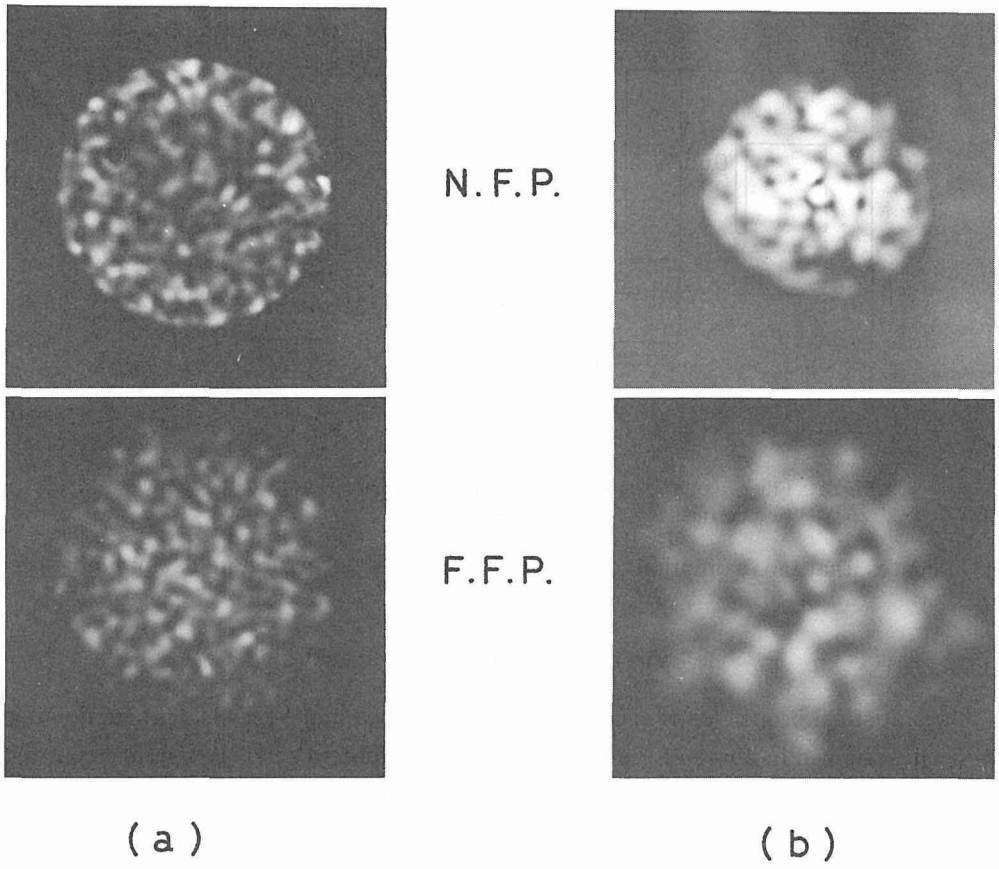

Fig. 2 Speckle patterns in the near- field (upper) and far-field (lower) regions from (a) a step-index fiber and (b) a graded-index fiber.

increase of the wavelength reduces the number of speckles and that a step-index fiber exhibits more speckles than a graded-index fiber because half the modes supported by the step-index fiber fails to exist in the graded-index profile[18].

Figure 2 (a) shows the typical examples of speckle patterns produced in near- field (N. F. P.) and far-field (F. F. P.) diffraction regions from a step-index fiber which has a 60 μm core diameter and a 0.20% relative index difference with the index valley of 6μm in thickness and 0.65% in depth between core and cladding. Figure 2 (b) shows typical examples of the near-and far-field speckles from a graded-index fiber having 50 μm in core diameter and 0. 34% in relative index difference with the index valley similar to that of the step-index fiber. The geometries of step-and graded-index fibers are illustrated in Figs. 3 (a) and (b). A comparison of Figs. 2 (a) and (b) shows that the characteristics of speckles are somewhat different from each other and that, as expected from mode dispersion, the speckles from the step-index fiber have a fine structure both in the near and the far fields in comparison with those from the graded-index fiber. It is also interesting to note that there is some degree of similarity between the near-and far-field speckles since the field distributions of the far-field pattern are given by a Fourier transform of the field over the exit face of the fiber[19]. This

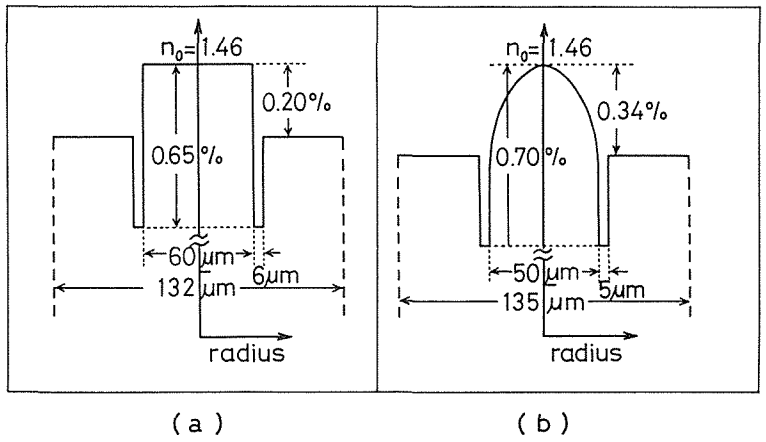

Fig. 3 Fiber geometries of (a) a step-index and (b) a graded-index multimode fibers.

fact indicates that an azimuthal dependence of modal structure holds in both speckle patterns[20].

3. First-order statistics of speckles

The statistical properties of speckle patterns produced in the far-field diffraction region have been examined in terms of the probability density function and the average contrast of the speckle intensity at a single point of the region. Imai et al[7-10]. studied the dependence of the statistics of speckles on the species of the fiber sample, the guide length of the fiber, and the lateral position in the far-field speckle pattern. More recently, Tsuji et al[11,12]. investigated the variation of the speckle patterns in a graded-index fiber with misaligned coupling and joints. The statistical approach was taken by analyzing the time-varying speckle intensity produced by vibrating the fiber, instead of scanning the spatial intensity distribution of the static speckle pattern[12]. The average contrast is defined as a ratio of the standard deviation to the average mean of the speckle intensity variation :

$$V=\langle\Delta I^2\rangle^{1/2}/\langle I\rangle=[\langle I^2(t)\rangle-\langle I(t)\rangle^2]^{1/2}/\langle I(t)\rangle \tag{4}$$

where I (t), $\langle I(t)\rangle$ and $\langle I^2(t)\rangle$ denote the time-varying speckle intensity, its mean and mean-square values, respectively.

The experimental setup of measuring the average contrast is shown in Fig. 4. The laser light emitted from a He-Ne laser of wavelength 6328Å, reflected at a half mirror M, and transmitted through a polarizer P is focused by a 4X microscope objective L to a nearly 20 μm spot size. The sample short-piece fiber is placed in a V-channel fiber

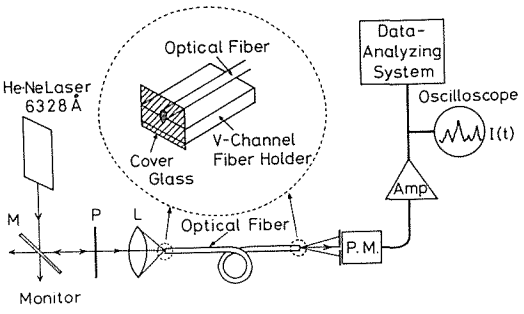

Fig. 4 Experimental setup used to measure the probability density function and the average contrast of speckle patterns.

holder filled with liquid paraffine of index n=1.47 and is mounted on a mechanically controllable stage in three dimensions. The radiation pattern produced by the laser light passing through the fiber is observed in the plane about 10 cm apart from the fiber exit end and detected by a photomultiplier (PM) with a 100 $\mu m\phi$ pinhole aperture. The time-varying speckle intensity from the PM is sampled at the rate of 4 msec and processed by a data -analyzing system consisting of an AD converter and a pulse-height analyzer. The sample rate is chosen appropriately to cover the fastest variation of the signal and a total of 10,000 samples is taken at every measurement.

Figures 5 (a) and (b) show the measured probability density functions of the speckle intensity, as a function of the fiber length, produced from a step-index and a graded-index fibers of Figs. 3 (a) and (b). Figure 5 (a) shows that the probability density function changes its form from a negative-exponential type to a degraded shape of low peak with an increase of the guide length of the step-index fiber. On the other hand, a Gaussian-like distribution of the probability density function is also observed in Fig. 5 (b) for the graded-index fiber. The Gaussian type is considered to correspond to the speckle patterns with a low contrast[13].

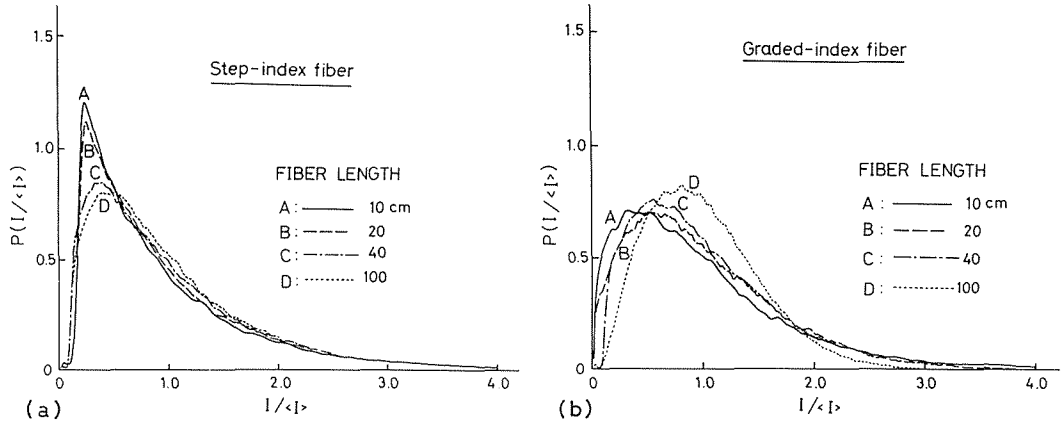

Fig. 5 Probability density functions of the speckle intensity produced from (a) step-index and (b) graded-index fibers with various lengths.

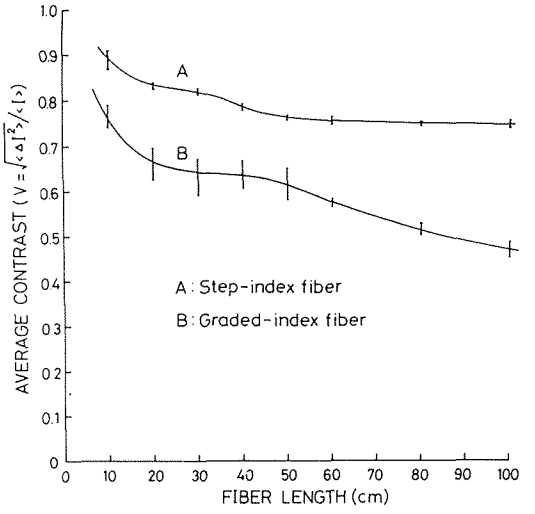

Fig. 6 Average contrast of speckle patterns as a function of the fiber length. The curve A stands for step-index fibers and the curve B stands for graded-index fibers. The vertical lines on the curves denote an error bar.

The speckle contrast obtained from these probability density functions is plotted in Fig. 6 as a function of the guide length. The dependence of the contrast on the guide length is explained from knowledge of modal dispersion. High contrast of the speckle pattern from the step-index fiber with a short length results from interference between only low-order modes excited by a laser beam. In due course of light propagation in an optical fiber higher -order modes take part in interference with the lower-order modes. This effect degrades the speckle contrast since such an interference plays a dominant role of averaging speckle patterns[7]. The average contrast produced from the graded-index fiber is almost constant over the guide length because the interference still takes place at a relatively long distance due to small waveguide dispersion. The speckle contrast of the graded-index fiber, however, is lower than that of the step-index fiber. This is due to the fact that the dominant Gaussian mode is mainly occupied at the central portion of the far-field diffraction region of light radiated from graded-index fibers.

The lateral variation of the speckle contrast is shown in Fig. 7 for two short pieces of 40 cm and 80 cm long step-index fiber. The high contrast remains unchanged at the periphery of the far-field diffraction pattern and, then, decreases in the neighborhood of acceptance angle of an optical fiber since the radiated light intensity diminishes rapidly near that angle. Comparing the curves of 40 and 80 cm in length, the contrast produced from the 40 cm long pieces is always higher than that of 80 cm long pieces and takes a maximum far away from the center axis. The behavior of speckle contrast variation along the lateral distance can be also explained from the evolution of modal structures in an optical fiber[8]. The average contrast of the speckle pattern is lowered on the axis since the specular intensity of HE_{11} mode is dominant, which is excited by an incident Gaussian beam. At the lateral position located away from the axis, the specular intensity decreases relatively to the increase of higher-order modes and the high contrast is attained due to the diffuse intensity consisting of the higher-order modes. As a result, the maximum contrast shifts toward the center axis for a long fiber of 80 cm.

The evolution of modal structures in a multimode optical fiber has been found to affect significantly the speckle pattern[21]. By means of a mode scrambler consisting of sinusoidally serpentine bends mode-coupling or mode conversion can be externally induced in an optical fiber[9]. It may be seen from the experimental result that the contrast decreases inversely with the increase of a half width of the far-field diffraction pattern. As the bending number of the mode scrambler increases, the speckle contrast approaches a certain constant low level where a steady state of mode redistribution is achieved as seen in Fig. 8.

It is well known that the visibility of speckles depends strongly on the coherence time or the spectral bandwidth of a light source as well. The maximum degree of spatial coherence[22] at the output of an optical fiber remains unchanged at the entrance if the light source bandwidth δf and the maximum transit time difference δt for all guided modes are such that[4-6]

$$\delta f \cdot \delta t \ll 2\pi \tag{5}$$

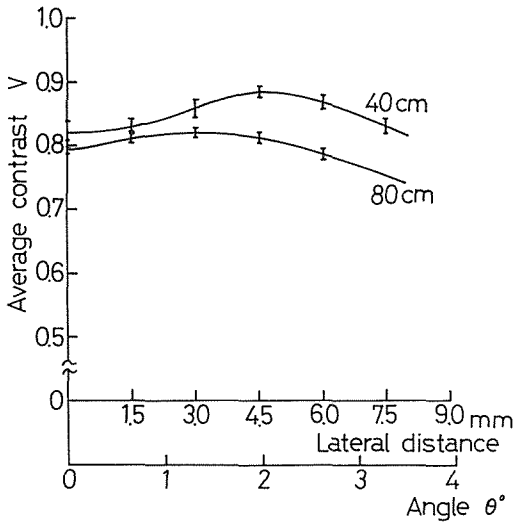

Fig. 7 Off-axis speckle contrast plotted as a function of the lateral distance or the angle θ for different lengths of a step-index fiber.

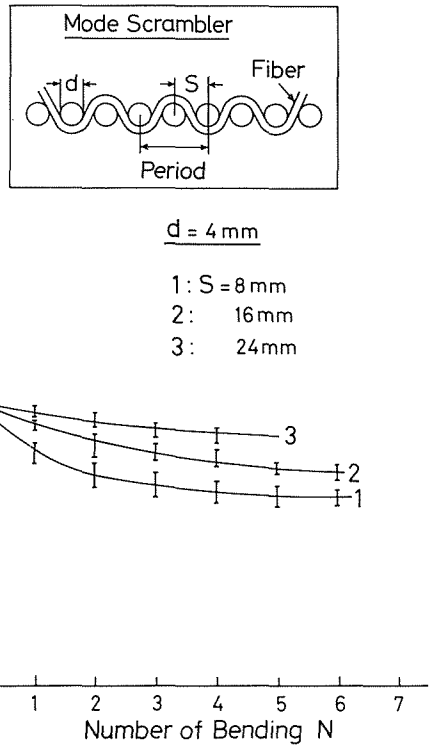

Fig. 8 Average contrast as a function of the number of bendings of mode scrambler utilizing sinusoidal, serpentine bends of fiber which is schematically shown above.

or, alternatively,

$$L \ll L_c = Cn_2/n_1(n_1 - n_2)\,\delta f, \tag{6}$$

where C is the light velocity in vacuum, L is the guide length and L_c denotes the critical length at which modes do not interfere with each other. In other words, the speckle patterns smear out at the exit end of the fiber exceeding the length L_c since the total pattern is provided by the sum of the intensities of independent modes. The relation of Eq. (5) or (6) holds generally true for a gas laser source and the fiber length used in interferometric application. However, a semiconductor laser source, which is much more suitable for a compact optical measuring system, possesses a somewhat broad spectral bandwidth. The speckle pattern produced by AlGaAs injection laser (Hitachi HLP laser) operating at 0.84 μm in wavelength has been also investigated by the author[10]. The spectral behavior of the injection laser is measured as a function of injection current as shown in Fig. 9. The single longitudinal mode oscillation is observed at the injection level as high as twenty percent above the threshold current I_{th}. When the injection current is 70mA that is less than I_{th}, the spectral half width is measured to be 50Å, which is not the lasing spectrum but that of spontaneous emission. The variation of speckle contrast with respect to the guide length of a step-index fiber is shown in Fig. 10 for a variety of injection currents. The contrast does not indicate a uniformly decreasing tendency for an injection current larger than I_{th} ; it decreases rather abruptly at the length larger than 30 cm up to 100 cm.

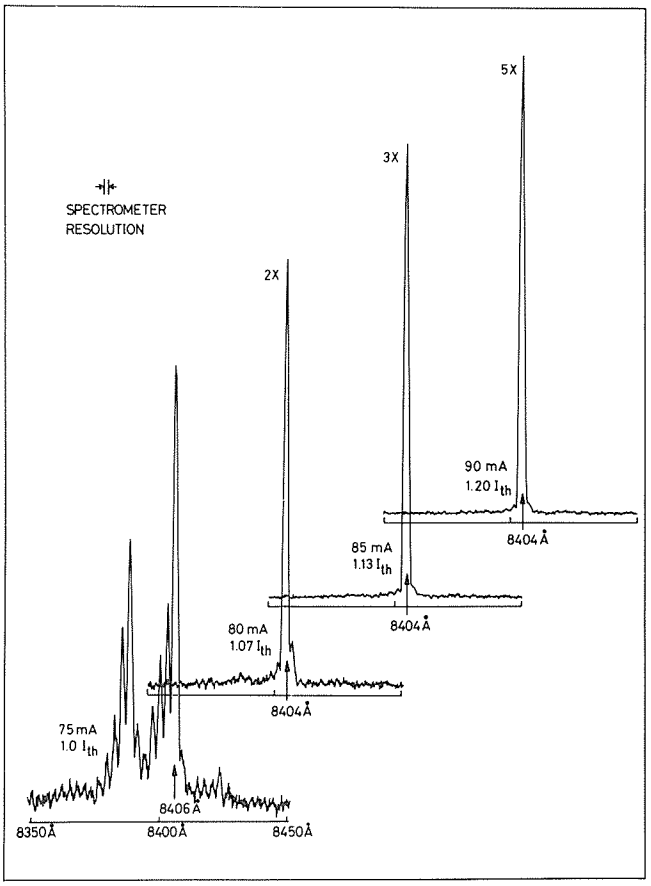

Fig. 9 Emission spectra of a GaAlAs laser diode at various injection currents under cw operation.

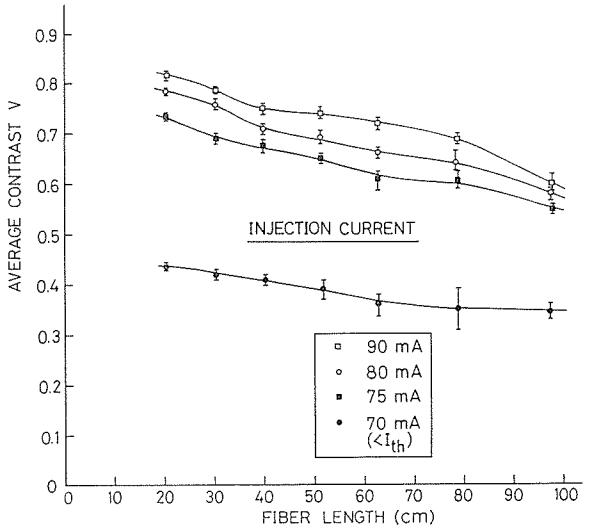

Fig. 10 Average contrast of speckle patterns for various injection currents of a laser diode.

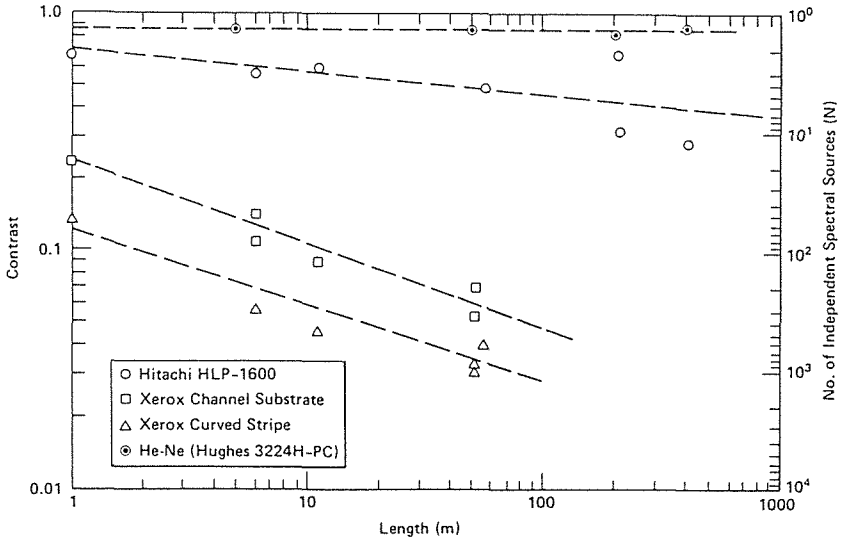

Fig. 11 Average contrast of speckle patterns versus guide length of step-index fibers illuminated by various sources. The broken lines represents approximate fits to the data[23].

The statistical analysis of speckle patterns for a relatively long fiber has been conducted by Rawson et al.[23] by scanning the exit face of the fiber. The average contrast of speckles produced from both a graded- and a step-index fibers illuminated with various sources is measured as a function of the fiber length over one hundred meters. Some results are demonstrated in Fig. 11. It is found that high contrast persists in a long length of the graded -index fiber excited by a single or a near-single wavelength source such as the He-Ne laser and the Hitachi injection laser. Conversely, the speckle contrast for the source of a broad spectrum is lowered even at short fiber lengths.

4. Second-order statistics of speckles

Although the first-order statistics of speckles are sufficient to describe the fluctuations of brightness in the near- and far-field planes, second- and higher-order statistics are necessary to describe other fundamental properties of speckles such as coarseness of its spatial structure. As shown in the photographs of Fig. 2, the speckle pattern is, in general, statistically non-stationary and its statistical properties are space-variant across the fiber core. As far as the step-index fiber with all guided modes equally excited is concerned, a simple assumption of space-invariant case is consistent with the measurement[23,24].

Assuming that the average size of speckles is much smaller than the core diameter of optical fiber, the exit end face may be regarded approximately as a spatially incoherent source, where spatial coherence is defined in an ensemble average sense. According to the Van Cittert-Zernike theorem[22,25], the normalized power spectral density of the speckle pattern, which was first derived by Goldfisher[1] using the conventional speckle theory, yields

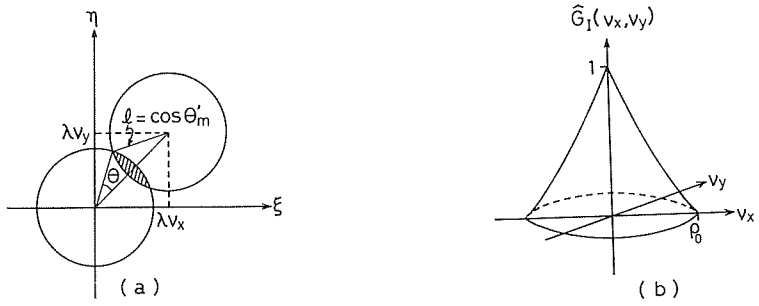

Fig. 12 (a) Overlap area to calculate the two-dimensional power spectral density and (b) power spectrum distribution ("Chinese-hat function") $\hat{G}_I(\nu_x, \nu_y)$ of Eq. (8).

$$\hat{G}_I(\nu_x, \nu_y) = \frac{\int_{-\infty}^{\infty}\int_{-\infty}^{\infty} R(\xi, \eta) R(\xi - \lambda\nu_x, \eta - \lambda\nu_y) d\xi\, d\eta}{\int_{-\infty}^{\infty}\int_{-\infty}^{\infty} R^2(\xi, \eta)\, d\xi\, d\eta}, \tag{7}$$

where $R(\xi, \eta)$ is the angular distribution of light intensity incident upon or emerging from the fiber end face, λ is the wavelength in the medium, and ν_x, ν_y are the spatial frequencies in each direction as illustrated in Fig. 12 (a). For the sake of convenience, $G_I(\nu_x, \nu_y)$ has been normalized to produce unity at $\nu_x = \nu_y = 0$. Thus, the two-dimensional power spectral density is proportional to the autocorrelation function of the apparent angular distribution of light emerging from the fiber output. Assuming that the fiber radiates a uniformly bright cone with an abrupt cutoff which is the case of a step-index fiber, the two-dimensional power spectrum becomes the so-called Chinese-hat function which is often abbreviated by "chat"[23] :

$$\begin{aligned}\hat{G}_I(\nu_x, \nu_y) &= \mathrm{chat}(\rho/\rho_o) \\ &\equiv \frac{2}{\pi}[\cos^{-1}(\rho/\rho_o) - (\rho/\rho_o) \\ &\times (1-(\rho/\rho_o)^2)^{1/2}], \quad \rho \leqq \rho_o, \end{aligned} \tag{8}$$

where $\rho = (\nu_x^2 + \nu_y^2)^{1/2}$, $\rho_o = 2 \sin\theta_m/\lambda$, and $\theta_m' = \pi/2 - \theta_m$ is the fiber critical angle. The behavior of $\hat{G}_I$ is schematically shown in Fig. 12 (b). In the experiment, a projection of the two-dimensional power spectrum onto the ν_x axis is measured by a linear detector array of 256 elements and the resultant

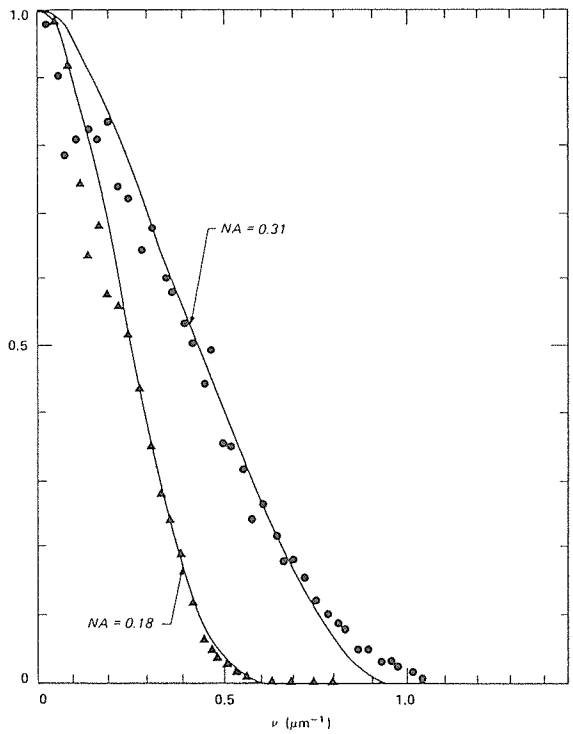

Fig. 13 Measured spatial power spectra for a large NA (core diameter 100 μm, length 1.1 m, NA=0.31) and a small NA (core diameter 90 μm, length 4.1 m, NA=0.18) fibers[24].

power spectra are calculated by taking a Fourier transform on each scan. Typical results of spatial power spectra are shown in Fig. 13 for different fibers with large and small NA. The solid lines denote theoretical curves calculated using Eq. (8) with the measured values of the fiber NA. It can be seen that the agreement between theory and experiment is reasonably good except for the experimental values of a small spatial frequency. The slight differences are likely to be due to deviations of the actual far-field distribution from the theoretically assumed cylindrical distribution[24].

5. Dynamic speckle and modal noise

In a fiber-optic system, the presence of speckles at the fiber exit end can cause fluctuations of the total guided power when the fiber is jointed to another similar fiber with an axial misalignment or a separation of the fiber ends as shown in Fig. 14. The loss originating from an imperfect joint depends strongly on the amount of offset and, in more precisely, it depends on the fraction of speckles falling within the core of the second fiber. Thus, the speckle-sensitive loss suffers temporal variations with changes in source wavelength and/or with physical distortion such as temperature and mechanical movement of the fiber since the speckle pattern varies in time and space due to these distortions. This effect has been recently observed by Epworth[14–16] and called a "modal noise".

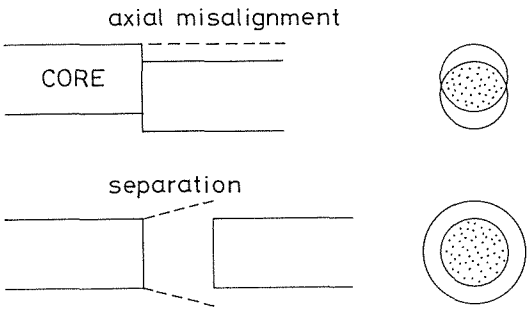

Fig. 14 Diagram of axial misalignment and end separation at the fiber-to-fiber joint. The schematic view of near-field speckles is also shown for each case.

5.1 Open speckle pattern

When we are concerned with modal noise properties we must examine whether core-guided light can couple with the cladding mode of the fiber at the mode-selective loss such as a misalignment. There are two statistically different regimes of speckle patterns ; one is termed the open regime and the other is the closed regime. Its terminology was first introduced by Hill et al [26,27]. Statistically closed speckle patterns are characteristic of an electromagnetic field of the core-guided light which does not exchange with the fields of cladding modes. In contrast, when such energy exchanges occur it becomes statistically open speckle patterns.

Let us consider the exit end of the fiber through which a large number of modes propagates. If the amplitude and phase of the different modes fluctuate independently at this plane, the dynamic speckle pattern is a random process. Provided that the relative phases of modes are uniformly distributed over a 2π interval, it can be shown that the instantenous intensity of each linearly polarized component of the field is a random variable having a negative-exponential probability density function[13]. Assuming that the end cross-section of the fiber is divided into many elementary areas in such a way that each of them

can be regarded as the speckle cell which is approximately the square of Δx (Eq. (1)). Then, the characteristic function of the probability density function P (I) crossing a finite area of the core is given by [28]

$$\phi(jv)=\prod_k \frac{1}{(1-jv\langle I_k\rangle)^{2m_k}}, \tag{9}$$

where $\langle I_k\rangle$ is the mean intensity of the k-th speckle cell and m_k is the number of the cells having the same value of $\langle I_k\rangle$. The factor 2 in the exponent takes into account the two polarization states of the transmitted light. The corresponding probability density function is obtained by inverse Fourier transforming Eq. (9) ; the mean value and the variance can be evaluated as $\langle I\rangle=\sum_k 2m_{\tilde{k}}\langle I_{\tilde{k}}\rangle$ and $\sigma^2(L)=\sum_k 2m_{\tilde{k}}\langle I_{\tilde{k}}\rangle^2$. Defining the signal-to-noise ratio as the mean divided by the standard value, we obtain for light intensity I (r) falling within a circular area having radius $r\leqq a$ (a=core radius) as[28,29]

$$\langle I(r)\rangle/\sigma(I)=(r/a)N^{1/2}, \tag{10}$$

where N is the number of modes propagating in the fiber. It is assumed in Eq. (10) that $\langle I_k\rangle$ is constant for every speckle cell and that the respective cell is mutually independent of each other. In the presence of some correlation or mode-coupling among guided modes, the signal-to-noise ratio has been analyzed and expressed in a rather simple form[30].

5. 2 Closed speckle pattern

As discussed previously, the statistics of the light transmitted through a limited aperture for the closed regime is more complicated since the speckles are interdependent from each other. However, Goodman and Rawson[29] and Tremblay et al.[27] independently have derived a rigorous expression for the probability density function of the transmitted light. These functions are a beta density distribution in the statistics literature and a transformed gamma distribution, respectively. The resultant ratio of the mean to the standard deviation in the latter case is deduced from the fundamental perspective and yields[26,27]

$$R=[n/(1-n/N)]^{1/2}, \tag{11}$$

where N is again the total number of guided modes which may be equivalent to the maximum number of degrees of freedom in the speckle distribution[26]. This is approximately given by $N=V^2/2$ for a step-index fiber and $N=V^2/4$ for a graded-index fiber where $V=ak(NA)$ is the normalized frequency of the fiber[17]. On the other hand, n represents the number of degrees of freedom in the transmitted portion of light as illustrated in Fig. 14 and is related to decibel loss at the fiber-to-fiber joint by

$$n=N\times 10^{-(dB\,loss/10)}. \tag{12}$$

Typical results of simulation experiment on modal noise caused by a misaligned connector are shown in Fig. 15. Squares and circles in the figure denote experimental points associated with a graded-index fiber of Fig. 3 (b) having different lengths of 1.9m and 6.5m before and after the misaligned joint. It is found that the theoretical curve is in good agreement with

the plots except for those of a small coupling loss where the predicted level is somewhat lower than the experimental values. This discrepancy is due to the presence of cladding modes in the second fiber since they can propagate without a large amount of loss. In the theoretical analysis of modal noise problem, careful discussion of the assumptions and approximations which went into the model of a misaligned connector is required to predict the accurate signal-to-noise ratio[31,32].

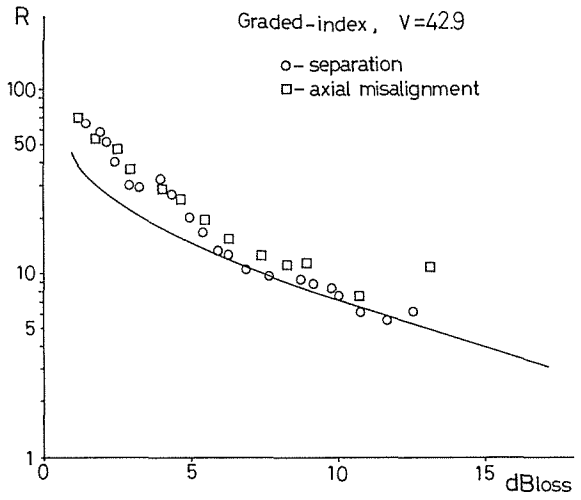

Fig. 15 The ratio R of the average intensity to the standard deviation of transmitted light as a function of coupling loss at the fiber joint. The solid line represents the theoretical curve of Eq. (11).

As is apparent from Eqs. (10) and (11), the signal-to-noise ratio in both cases decreases with the decreasing number of guided modes. The worst case occurs in a two-mode fiber in which the lowest-order and the next low-order modes only are present. The predicted level of total power fluctuations has been also determined for a quasi-single mode fiber operated slightly above the cutoff of the next mode[33,34]. Even in a true single-mode fiber, it is actually bimodal (two-mode) from the viewpoint of two orthogonal states of polarization which the nominally circular-core fiber can support. When the misalignments of both transverse offset and axial inclination exist in a single-mode fiber connector, the loss of a connector depends on the polarization as well[35]. This fact gives rise to the polarization-dependent modal noise provided that dynamic speckles are induced in the fiber core before the connector[36,37]. Furthermore, if elements with polarization-dependent loss such as a diffraction grating[38] and a polarizer[39] are inserted in a single-mode fiber link, fluctuations of the state of polarization will produce intensity noise called "polarization noise". The polarization noise originating from angular misalignment of the axis in the coupling of two birefringent fibers and/or the axis of the input fiber has been intensively investigated by the author[40].

5.3 Wavelength-dependent noise

In an actual optical communication system, the most serious causes of modal noise are fluctuations in oscillating frequency of a laser diode[41]. The coupling efficiency at the fiber-to-fiber connector has been analyzed as a function of the emission frequency of a laser source[42,43]. The transmitted power of a typical multimode fiber through the connector is highly sensitive to even a small shift of emission frequency[44]. Such a frequency shift occurs during laser modulation since direct modulation of a laser diode modulates not only the emitted power but also the wavelength[14,15]. More recently, the speckle contrast for multimode fibers and, thus, the modal noise have been analyzed in terms of the impulse

response of the fiber and the power spectrum of the source[45]. It is interesting to note that laser sources with a large spectrum of narrow longitudinal modes may cause high speckle contrast and important modal noise over more than 1 km length in graded-index multimode fibers.

In order to obtain a quantitative understanding of the frequency dependence of modal noise effects, Rawson et al.[23,24] has defined a frequency correlation function that is similar to the spatial correlation function developed in Chap. 4. Taking a speckle theory approach to the problem of modal noise, the source frequency interval required to decorrelate the speckle pattern at the exit end of the fiber is given as a function of the fiber parameters of guide length and numerical aperture. This frequency correlation function of the speckle pattern is shown to be proportional to the 3-dB bandwidth of the fiber and is used to estimate the bandwidth of a multimode optical fiber[46,47]. Therefore, a simple measurement of speckle contrast yields the linewidth of laser sources or the bandwidth of short multimode fiber pieces by calibrating either the laser or the fiber[48].

6. Conclusion

We have reviewed the statistical properties of speckle patterns at the output end of a multimode fiber through which coherent light such as a laser beam propagates. This speckle pattern results from random interference among many guided modes with a slightly different velocity. Thus, the speckles in the near- and far-field regions may be regarded as a random process over its spatial distribution. Since the properties of speckle patterns are space -variant, the average contrast of speckles, i. e., the ratio of the standard deviation to the mean value of the speckle intensity variation, is determined across the core of a step- and graded- index fibers with various lengths. Consequently, it is confirmed that the evolution of speckle contrast along the guide length is related to mode conversion or mode-coupling between propagating modes.

Next, we have discussed dynamic speckles which vary in time due to changes in source wavelength and/or physical distortion of the fiber. The fluctuations of the speckle pattern, known as a "modal noise", are treated from two different regimes of speckle statistics. The modal noise is closely related to the coupling loss of a fiber connector and its signal-to-noise ratio is shown to decrease with an increase of the loss occurring at the imperfect joint for a typical multimode fiber. It should be noted that the statistical properties of speckle patterns, and thus the modal noise depend not only on mode dispersion of optical fibers but also on the emission characteristics of laser sources.

Acknowledgment

The author wishes to thank Prof. Y. Ohtsuka for his encouragement during this work. Thanks are also due to Prof. T. Asakura for his fruitful discussions on optical fiber speckles.

References

1) Goldfisher, L. I. : J. Opt. Soc. Am., **55** (1965) pp. 247−253.
2) Hioki, R. and Suzuki, T. : Japan. J. Appl. Phys., **4** (1965) p. 817.
3) Suzuki, T. : Japan. J. Appl. Phys., **6** (1967) pp. 348-355.
4) Crosignani, B. and Di Porto, P. : J. Appl. Phys., **44** (1973) pp. 4616-4617.
5) Crosignani, B., Daino, B. and Di Porto, P. : Opt. Commun., **11** (1974) pp. 178-179.
6) Crosignani, B., Daino, B. and Di Porto, P. : J. Opt. Soc. Am., **66** (1976) pp. 1312-1313.
7) Imai, M. and Asakura, T. : Optik, **48** (1977) pp. 335-340.
8) Imai, M., Iida, M. and Asakura, T. : Optik, **51** (1978) pp. 429-434.
9) Imai, M. and Asakura, T. : Opt. Commun., **30** (1979) pp. 299-303.
10) Imai, M. and Ohtsuka, Y. : Opt. Commun., **33** (1980) pp. 4-8.
11) Tsuji, T., Asakura, T. and Fujii, H. : Opt. Quantum Electron., **16** (1984) pp. 9-18.
12) Tsuiji T., Asakura, T. and Fujii, H. : Opt. Quantum Electron., **16** (1984) pp. 197-205.
13) Goodman, J. W. : *Laser Speckle and Related Phenomena* (edited by Dainty, J. C.), Springer-Verlag, New York (1975) pp. 46-54.
14) Epworth, R. E. : Proceedings of the Fourth European Conference on Optical Communication, Genoa (Sept. 1979) p. 492.
15) Epworth, R. E. : Technical Digest of the Topical Meeting on Optical Fiber Communication, Washington, D. C. (March 1979) p. 106.
16) Epworth, R. E. : Laser Focus, **17** (1981) pp. 109-115.
17) Gloge, D. : Appl. Opt., **10** (1971) pp. 2252-2258.
18) Gloge, D. and Marcatili, E. A. J. : Bell Syst. Tech. J., **52** (1973) pp. 1563-1578.
19) Kapany, N. S. and Burke, J. J. : *Optical Waveguides,* Academic Press, New York (1972) pp. 207-216.
20) Imai, M. : Trans. IECE Japan, **E 63** (1980) pp. 16-23.
21) Imai, M. : Radio Science, **16** (1981) pp. 555-561.
22) Born, M. and Wolf, E. : *Principles of Optics,* 5th ed., Pergamon Press, New York (1975) pp. 505-518.
23) Rawson, E. G., Goodman, J. W. and Norton, R. E. : J. Opt. Soc. Am., **70** (1980) pp. 968-976.
24) Rawson, E. G. and Goodman, J. W. : Proceeding of the Society of Photo-Optical Instrumentation Engineers, **243,** *Applications of Speckle Phenomena* (1980) p. 28.
25) Imai, M. and Ohtsuka, Y. : The Review of laser Engineering, **9** (1981) pp. 222-236 (in Japanese).
26) Hill, K. O., Tremblay, Y. and Kawasaki, B. S. : Opt. Lett., **5** (1980) pp. 270-272.
27) Tremblay, Y., Kawasaki, B. S. and Hill, K. O. : Appl. Opt., **20** (1981) pp. 1652-1655.
28) Daino, B., De Marchis, G. and Piazzolla, S. : Optica Acta, **27** (1980) pp. 1151-1159.
29) Goodman, J. W. and Rawson, E. G. : Opt. Lett., **6** (1981) pp. 324-326.
30) Daino, B., De Marchis, G. and Piazzolla, S. : Opt. Commun., **38** (1981) pp. 340-344.
31) Mickelson, A. R. and Weierholt, A. : Appl. Opt., **22** (1983) pp. 3084-3089.
32) Hjelme, D. R. and Mickelson, A. R. : Appl. Opt., **22** (1983) pp. 3874-3879.
33) Heckmann, S. : Electron. Lett., **17** (1981) pp. 499-500.
34) Imai, M. : Trans. IECE Japan, **E 66** (1983) pp. 248-249.
35) Gambling, W. A., Matsumura, H. and Ragdale, C. M. : Electron. Lett., **14** (1978) pp. 491-493.
36) Heckmann, S. : Opt. Lett., **6** (1981) pp. 201-203.
37) Epworth, R. E. and Pettitt, M. J. : Technical Digest of the Third International Conference on Integrated Optics and Optical Fiber Communication, San Francisco (April 1981) p. 58.
38) Hillerich, B. and Weidel, E. : Opt. Quantum Electron., **15** (1983) pp. 281-287.
39) Imai, M. and Ohtsuka, Y. : Opt. Lett., **10** (1985) pp. 423-425.
40) Imai, M. and Ohtsuka, Y. : Proceedings of the Second International Conference on Optical Fiber Sensors, Stuttgart (Sept. 1984) paper PD1.
41) Olesen, H. : Electron. Lett., **16** (1980) pp. 217-218.
42) Petermann, K. : IEEE J. Quantum Electron., **QE-16** (1980) pp. 761-770.
43) Petermann, K. and Arnold, G. : IEEE J. Quantum Electron., **QE-18** (1982) pp. 543-555.

44) Baack, C., Elze, G., Grosskopf, G. and Walf, G. : Proc. IEEE, **71** (1983) pp. 198-208.
45) Dandliker, R.. Bertholds, A. and Maystre, F. : J. Lightwave Technol., **LT-3** (1985) pp. 7-12.
46) Moslehi, B., Goodman, J. W. and Rawson, E. G. : Appl. Opt., **22** (1983) pp. 995-999.
47) Freude, W., Fritzsche, C. and Grau, G. K. : Appl. Opt., **22** (1983) pp. 3319-3320.
48) Freude, W., Fritzsche, C. and Shanda, L. : Proceedings of the Tenth European Conference on Optical Communication, Stuttgart (Sept. 1984) p. 216.